

RAIN CELL SIZING FOR THE DESIGN OF HIGH CAPACITY RADIO LINK SYSTEMS IN SOUTH AFRICA

P. O. Akuon^{*} and T. J. O. Afullo

School of Electrical, Electronic and Computer Engineering, University of Kwa-Zulu Natal (UKZN), Durban 4041, South Africa

Abstract—Rain cell size is an input requirement for rain-induced attenuation studies. It is useful in estimating the extent of a given radio link path that will traverse the rain medium in a given rain event. The “Synthetic Storm” approach, which requires 1-minute integration time data, is used to derive the proposed rain cell sizes for various climatic zones within South Africa. The conversion of the readily available 1-hour integration time rain rate data to the desired 1-minute rain rate is carried out first for some locations and then validated by the existing measurement data and proposed global conversion factors. By the use of rain-induced attenuation prediction equation for terrestrial links that requires rain cell size as input, contour plots of specific attenuation for two high bandwidth frequencies used in terrestrial link implementations is presented. Site diversity separation distance map is proposed as well from the link budget analysis for each location to achieve an all time link availability of 99.99% of time.

1. INTRODUCTION

There is a continual evolution of telecommunication technologies today partly as a result of the problems and limitations encountered in the use of high capacity radio links. Fibre optic transmission is an alternative for signal transmission praised for its high bandwidth transmission capability but is highly prone to accidental damage making it a comparatively insecure channel with rampant maintenance requirements expected. The growth in smart phones acquisition by subscribers is expected to increase the demand for services like Internet

Received 30 August 2011, Accepted 19 October 2011, Scheduled 1 November 2011

** Corresponding author: Peter O. Akuon (akuonp@yahoo.com, 210550793@ukzn.ac.za).*

connectivity, multimedia and video-streaming, and digital television thus increasing bandwidth demand. Therefore, there is rising need to fully utilize the microwave spectrum especially the 10 GHz and above. However, these frequencies are prone to undesired signal attenuation as they pass through precipitation due to their relatively small wavelengths. While the effects of precipitation agents have remained a major disturbance of the transmitted radio signals in terrestrial and satellite systems, the effects of rainfall are more significant. Therefore, rainfall attenuation studies have been of interest, particularly to radio link planners for signal transmission at millimeter wavelengths. There is need to model rainfall more fully by determining the size of rain cells for a given rain rate threshold and the growth of rain rates in order to achieve more accurate global attenuation prediction results. ITU-R [1] and many other authors including [2–6] have suggested the need for determination of the rainfall rate parameter, $R_{0.01}$, to obtain precise calculations involving attenuation studies. $R_{0.01}$, (mm/h) defined as the rainfall rate exceeded for 0.01% of time in a year, helps radio system engineers to predict the expected worst case rainfall attenuation that would occur at that percentage exceedance level. Values of $R_{0.01}$ can be obtained from the available rainfall rate data in ITU-R data bank or from long term local measurements. These values are dependent on the integration time of the measurement device in use. Many researchers [7, 8] have suggested the use of integration times of 1-minute as the most suitable. Rainfall studies in Africa [4–7, 9, 10] and South African region [11–13] have suggested the need for adequate rainfall data at 1-minute integration time, which are scarce. However, higher integration time data (hourly, daily and even, monthly) are available from many weather stations. Thus, the scarcity of 1-minute rainfall data requires conversion from higher integration time rainfall rate data obtained from the location under consideration by the use of suitable conversion techniques [8, 14–20]. An attempt is made to predict the expected $R_{0.01}$ values for South Africa by the use of the available 1-hour integration time data. Section 2 describes the conversion method adopted for this work based on power law relationship which is presently recommended by the ITU-R. The results obtained for the South African rain regions are then used to determine the equivalent rain cell diameter size in section 3. Based on an earlier work by the authors on terrestrial link attenuation prediction, the rain cell size model is used in section 4 to produce attenuation maps for the region. Section 5 presents the proposed separation distance mapping for site diversity in South Africa, a useful technique employed in rain attenuation alleviation methods.

2. INTEGRATION TIME RAINFALL RATE CONVERSION

The rain rate measurements used here are obtained from the Centre of Excellence (COE) in Howard Campus of the University of KwaZulu-Natal, Durban. The Joss-Waldvogel disdrometer set up at the centre is connected to a terminal computer which records 1-minute integration time data. The data is collected over a period of two years with minimal equipment outages. The hourly data for Durban and all other locations were obtained from the South African Weather Service (SAWS) data bank for a period of five years.

Rainfall rate conversion adopted here involves the process of converting rainfall rate values from a higher integration time to a smaller integration time. The conversion is unique to a particular region because it involves the geographical and climatic properties of a location. While notable methods of conversion have been developed [8, 10–19], it is interesting to note that some of these methods depend on the prevailing climatic factors. The rainfall rate conversion methods have been classified into three categories by Emiliani et al. [20] namely: physical-stochastic, empirical and analytical methods. In classifying the methods, they considered the modeling, procedural influences and physical processes involved in the rainfall rate conversion. ITU-R also specifies the power-law conversion law for some countries and regional maps exist showing regional values for $R_{0.01}$ (see ITU-R 837-5). It should be noted that the ITU-R method is empirical as it considers rainfall data within a location to derive conversion parameters. Interestingly, other empirical methods including that of Flavin [14] and Segal [15] are based on power-law conversion methods. This method was used by Ajayi and Ofoche [7] to derive rain conversion parameters in several locations in Nigeria. Owolawi et al. have introduced various rain rate conversion methods for application in the South African region: Hybrid, Linear, Power and Polynomial. The polynomial method was tested as the best method for the ten year, 5-minute rain rate data from 21 stations in South Africa [19, 21, 27].

The power-law conversion function in ITU-R 837-5 [1] is given by:

$$R_1(P_T) = \alpha [R_\tau(P_T)]^\beta \quad (1)$$

where α and β represent the conversion coefficients of the rainfall rates $R_1(P_T)$ and $R_\tau(P_T)$ at 1-minute and τ -minute integration times respectively at equal probabilities P_T .

Studies have shown climatic variations particularly between the Eastern Coasts and Western Coasts of South Africa [18, 21, 22]. In this work, we derive rainfall rate parameters α and β for Durban based

on empirical data and extend this relationship to other sites in South Africa. This approach caters for the variation of climatic conditions at several locations in South Africa. By utilizing the available 2 year, 1-minute rain rate data from the disdrometer, we simulate our conversion method, based on the power-law empirical method of Watson et al. [8] to determine our parameters for the various locations selected for this study.

The derivation of rainfall rate conversion factors for different locations is achieved by comparing the hourly data between Durban and other cities. Through this approach, we obtain regression coefficients α' and β' for the relationship between Durban and those cities. Consequently, we use (1) to compute the conversion factor for the 1-minute and hourly measurements for Durban at equal rain rate probability exceedances. From [1] the relationship is given as:

$$R_1 = \alpha' [R_{60}]^{\beta'} \quad (2)$$

where α' and β' are the regression coefficients obtained for Durban.

By comparing the respective hourly data between other cities and Durban at equal rainfall rate probability exceedances, we get another set of expressions with regression coefficients α'' and β'' as expressed in (3):

$$R_{60,X} = \alpha'' [R_{60,Durban}]^{\beta''} \quad (3)$$

where X represents the location being compared with Durban in the 1-hour data.

On the basis of (2) and (3), we obtain the values of α and β in Equation (1) by multiplying the regression coefficients in (2) and (3) thereby defining unique values for each location. Firstly, we use the derived coefficients for Durban to convert the hourly-data from other towns to their equivalent 1-minute values. Thus,

$$R_{1,X} = \alpha' [R_{60,X}]^{\beta'} \quad (4a)$$

where $R_{1,X}$ is the 1-min rainfall rate for a given town.

But since we have derived the relationships between the hourly data for Durban and those of other towns as expressed in (3), the 1-minute results obtained in (4a) are then transformed by the coefficients α'' and β'' to obtain the exact values for those towns. This way, we assume that the transformation of the hourly data between Durban and any other town give the same results that would be obtained if 1-minute data were transformed between Durban and any of the towns. This assumption is validated later with the comparison tests in Table 3. Thus, the new 1-minute rain rate value for any town is given as:

$$R_{1,X} = \alpha'' \left(\alpha' [R_{60,X}]^{\beta'} \right)^{\beta''} \quad (4b)$$

From (4b), the overall regression coefficients can then be defined as expressed in (4c) and (5):

$$\alpha = \alpha''(\alpha')^{\beta''} \quad (4c)$$

$$\beta = \beta''\beta' \quad (5)$$

We compare the hourly rain rate data for Durban to those of the other locations since the statistics of 60-minutes resolution data for different locations are more closely related than those of 60-minutes to 1-minute data. This process is repeated for four other locations in South Africa. Fig. 1(a) shows the equiprobable plot of corresponding rain rate values at 1-min integration time and 1-hour. The non-unity correlation coefficient, $R^2 = 98.95\%$ means that the conversion factor is adopted even though not all the points lie on the graph but it is considered adequate for this work. Fig. 1(b) is a cumulative distribution (CDF) graph for Durban site. The graph of $T = 60$ minutes is the measured 5-year, hourly rainfall data for Durban and the graph of $T = 1$ Minute is the measured 2-year, 1-minute rainfall data. The third graph is the CDF graph for $T = 60$ minutes multiplied by the derived conversion factors ($\alpha' = 6.3313$, $\beta' = 0.6837$).

From Fig. 1(b), it can be seen that the translation of the CDF curve ($T = 1$ Min translated from 1 hr curve) closely follows the curve obtained from the measured time series rain rate data ($T = 1$ Min). The 1-min data gives better resolution with the lowest rain rate of 0.01 mm/h while for the 1-hour data, the lowest rainfall rate of 0.2 mm/h is exceeded only 3.9367% of the time in a year. This results in a substantial loss of rain rate information in the 1-hour data. Also, the length (1 707 hours) of the 1-hr series data is far less than that of the 1-min series data (40 140 minutes), thus we consider the whole year period for the 1-hr series data including the dry spell periods in a year (see Ajayi et al. [4, 7]) while only the rainy days for 1-min series data are considered.

The loss of data and the difference in the time period explain the reason why the distribution for the measured 1-min data is much higher than that of the 1-hr for the rain rates below 6 mm/h as depicted in Fig. 1(b).

Figure 2 illustrates the CDF plots of the measured 1-hour and 1-minute data from Durban, measured 1-hour data from Richards Bay and converted 1-minute data for Richards Bay. The conversion factors for all the climatic locations considered in this work are listed in Table 1.

Since 5-year rainfall data are collected in hourly basis, the CDF of rainy days alone would result in limited statistics. In some cases,

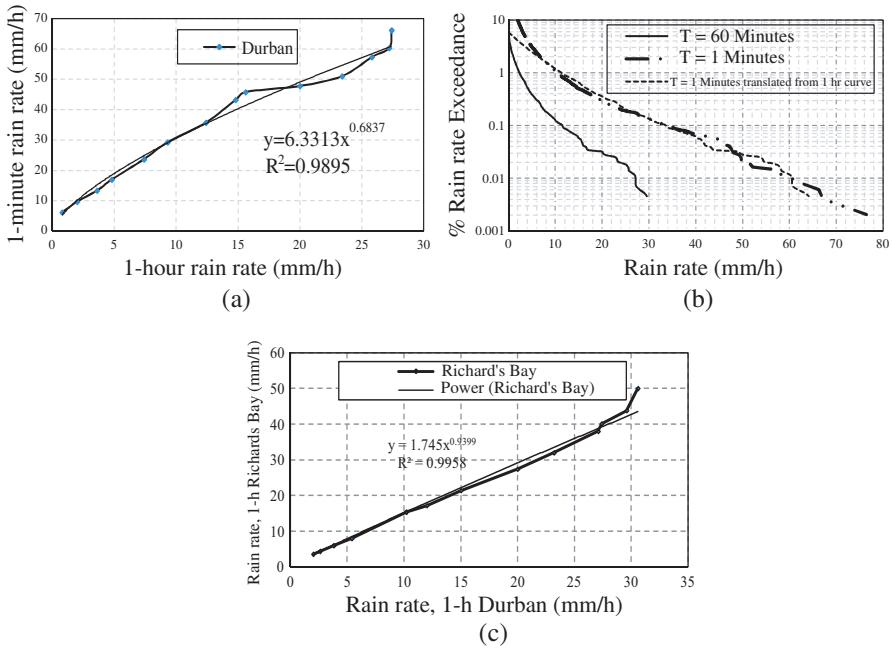


Figure 1. Rain rate conversion technique for Durban. (a) 1-h to 1-min conversion plot for Durban. (b) Rain rate CDF, Durban for 1-min and 1-h. (c) 1-h to 1-h conversion between Durban and Richard’s Bay.

Table 1. Rainfall rate integration time power law conversion coefficients for four climatic locations in South Africa.

LOCATION	LON	LAT	α	β	R^2
DURBAN	29° 97'	30° 95'	6.3313	0.6837	0.9895
PRETORIA	25° 73'	28° 18'	5.0935	0.6743	0.9830
PIETERMARITZBURG	30° 40'	29° 63'	6.1143	0.8393	0.9847
RICHARD’S BAY	32° 60'	28° 48'	9.8863	0.6426	0.9847
ILE-IFE NIGERIA [11]	04° 31'	0° 30'N	11.565	0.7982	-

the highest recorded rainfall rate would seem to occur 0.1% of time. This means that the 1-hour statistics present significant loss of vital data required in rainfall rate modeling. In order to solve this, we have included dry spell period in each year for the 1-hour integration time data but retain the exact rainy days statistics for the 1-minute data collected from the disdrometer. This has enabled us to achieve

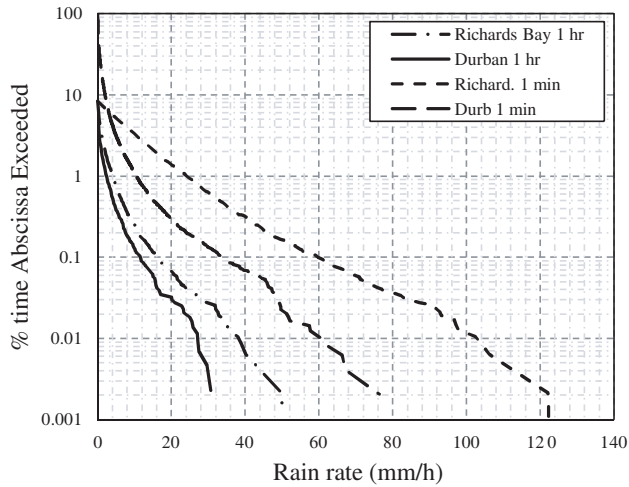


Figure 2. Rain rate CDF for Durban and Richard’s Bay for 1-hr and 1-min integration time.

lower than 0.01% of time in the 1-hour data that can then be related to the 1-minute data for conversion model to be achieved. This approach including the dry spell period in the 1-hour data was used by Ajayi et al. to improve the resolution of data with higher integration time, and the same was applied by Sakar et al. in India [4]. Based on rainfall measurements in Ile-Ife, Nigeria, between September 1979 and December 1981 by the use of a fast response rain gauge with an integration time of 10 seconds, Ajayi et al. produced a table for the power law conversion coefficients. By linear extrapolation, it has been determined that $\alpha = 11.565$ and by logarithmic extrapolation, $\beta = 0.7982$ for conversion from 60 minutes integration time data [4, 11]. Since Ile-Ife is a tropical site, while Durban and Richard’s bay are subtropical, it is expected that the conversion factor for Ile-Ife will be higher than those in South Africa. This is depicted in Table 1.

In order to validate the conversion method employed in this work, the results of the proposed 1-min rainfall rate data are compared to those obtained from global coefficients as contained in the work of Emiliani et al. [20]. Table 2 lists the power law coefficients q (amplitude) and r (power) where the 1-min data is obtained from measured 60-min data. In their work, they presented the percentage relative deviation of the coefficients for different climatic zones: temperate, cold, tropical and global. In this work, we use the global coefficients.

Table 3 shows the results obtained from the measurements,

Table 2. Global rainfall rate (60-min to 1-min) integration time coefficients [20].

Global coefficients	$q = 0.509$	$r = 1.394$
Max. rel. deviation	48%	17%
Min. rel. deviation	-52%	-15%

Table 3. Comparison of the proposed conversion factors with global coefficients.

LOCATION	DATA	% of TIME		
		1%	0.1%	0.01%
DURBAN	1-h measured	2.20	11.40	27.20
	1-min measured	10.49	34.45	60.35
	Proposed (1-min)	10.85	33.42	60.56
	Emiliani et al. (1-min)	2.63	29.20	63.65
PRETORIA	1-h measured	1.60	9.80	21.20
	Proposed (1-min)	6.99	23.73	39.93
	Emiliani et al. (1-min)	1.65	23.40	44.20
PIETERMARITZ BURG	1-h measured	2.20	13.20	30.60
	Proposed (1-min)	11.48	46.13	89.71
	Emiliani et al. (1-min)	2.45	39.48	88.77
RICHARD'SBAY	1-h measured	4.00	16.20	38.00
	Proposed (1-min)	24.09	59.19	102.38
	Emiliani et al. (1-min)	6.20	54.22	124.19

proposed method and those obtained from the coefficients in [20]. The equiprobable rainfall rates were plotted between 1% and 0.01% of time both for the proposed method and those of [20]. It is evident that within the relative deviation levels of Table 2, the values compare closely for the rain rates between 0.1% and 0.01% of the time. At 1% of the time, the proposed method results in a more accurate prediction for the measured 1-min data in Durban. The global coefficients show a larger difference at higher percentage exceedance e.g., 1% since the compared values of rain rate of the 1-h data (5 years) and 1-min data (2 years) vary considerable at these levels. The ITU-R P.837-5 [1] suggests that conversions from 30-min to 1-min with an average absolute difference of 5.72 mm/h for the measurements is acceptable, therefore the resulting differences in rainfall rate values in Table 3 should be acceptable as well.

3. DERIVATION OF RAIN CELL SIZES

A rain cell can be defined as the area bound by a given rain rate threshold and above. We take a circular assumption of shape to derive cell diameter size statistics for South Africa. In our earlier work [24], we gave detailed procedures used in this process for Durban. The same approach is used here to determine rain cell sizes for three other regions within South Africa. The point rain rate time series data is converted to distance series data by multiplying the duration taken by rain form by its appropriate advection velocity. This conversion is made for all the rain events in the measurements. This procedure is called “Synthetic Storm” technique which was initially introduced in 1975 by Drufuca and has been used by many authors e.g., Pawlina et al. and Begum et al. to derive rain cell size statistics around the world [25–28]. The data availability consists of 2 year, 1-min integration time series disdrometer data (518 rain events with rain rate of at least 3 mm/h, total of 669 hours of rainfall) and 5 year, 1-hr integration time series rain gauge data (466 rain events with rain rate of at least 3 mm/h, total duration of 1707 hours). The rain rate thresholds used to group the data are the 3, 12 and 20 mm/h. Any given rain event exhibits a continuous change in rain rate with time as the rain moves across a given area. The drop diameters also keep on changing, a phenomenon which results to non-uniform speed of advection of rain form. However, the knowledge of an average advection velocity for each portion of a constant rain rate within one minute would be adequate. Some research has shown that intense convective rain forms move faster than less intense ones. Though the rain form is expected to move at the 700 mb wind speed, this is not the case and the correlation of the two has been shown to be poor. Radar scans have also been used to measure the translation velocity of rain cell structures which provide relatively good result. The Doppler speed detection only scans rain structures that move towards or away from the radar and result in prediction of lower velocity values [28, 29]. By the use of attenuation statistics in [24], we were able to estimate typical advection velocity of the stratiform rain forms with rain rate, $R < 12$ mm/h as 6 m/s and those of the convective rain forms as 10 m/s. The output distance data for each class are then processed statistically to find their cumulative probability distribution. Goldhirsh [26] showed that with CDF of rain cell extensions, the rain rate-distance relationship can be derived from the graphs at a given percentile level (with power law coefficients u and v). If all the occurrences of rain events are to be taken into account, then the rain cell size model thus determined must be able to predict the largest cell area for a given rain rate threshold. This is

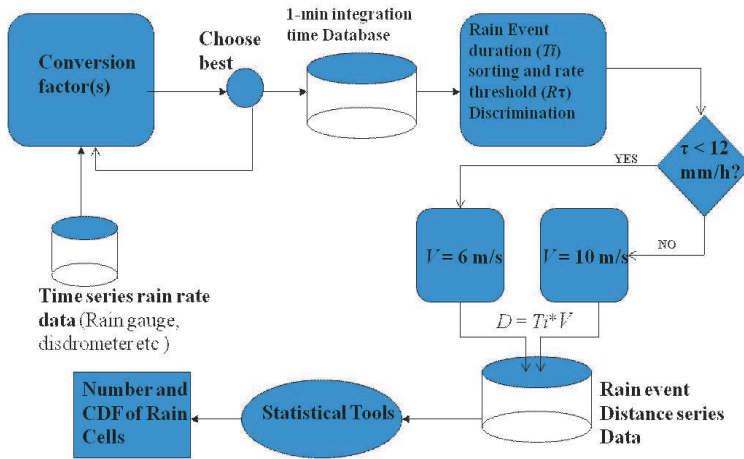


Figure 3. Rain cell size CDF production process from point rain rate.

done by plotting the graph of the equiprobable distances in the classes against the respective lower bounds of rain rates and fitting a power law relationship between those rain rates and the equiprobable cell diameters. The resulting equation produces the equivalent rain cell diameter size model. The chart of Fig. 3 describes the logical data exchange between the measurements and the rain cell size distribution statistics.

The data base of rain rate time series stores the data specified by different integration times and time period constraints, e.g., 5 years. To convert the data to recommended 1-minute series, a viable method is iteratively chosen from a list of conversion models available. The high resolution (1-min is recommended) rain rate data is then separated into rain events. For each rain event, rain rate thresholds are chosen. There are so many cells that result from the data when rain rate thresholds below 3 mm/h are included in the study and this is likely to skew the resulting distribution. Radar scans have also shown that the cells may not obey the circular shape assumption. The rain cells from higher rain rate thresholds are also few which may lead to unstable distribution [28, 29]. We apply threshold classes for 3, 5, 12 and 20 mm/h. The rain forms are classified into two: stratiform ($R < 12$ mm/h) and convective ($R \geq 12$ mm/h).

For each rain event, if the portion of rain rate is stratiform, then the distance is computed by multiplying the total time taken by that portion by a velocity value of 6 m/s. Otherwise, for convective cell areas, a velocity of 10 m/s is applied. This procedure is repeated for all

the threshold values considered and the resulting distances are stored separately. The probability distribution, PDF of the distances would result in rain cell number distribution while the CDF easily predicts the rain cell size distribution.

This procedure is carried out to derive the equivalent rain cell size for Durban area by the use of the ITU-R-recommended measured 1-min integration time data. The result of the rain cell size distribution is shown in Fig. 4(a). After this, we derive the equivalent cell size for Durban area by the use of the measured 1-h integration time data: See Fig. 4(b). However, due to the limited resolution in the data, it is hard to compare the resulting cell size distribution with those derived from the 1-min plots. For example, in the 1-h measurements, when the rainfall rate is 0.2 mm/h with a velocity of 6 m/s (21.6 km/h), the cell size generated would be 21.6 km (1 hour by 21.6 km/h). For the convective rain forms with velocity of 10 m/s (36 km/h), the cell size would be 36 km. In an attempt to resolve this, we therefore convert the 1-h time series data by the use of conversion factors in Table 1 to obtain the rainfall rate values that would produce the same CDF as the measured 1-min integration time series data. Conversely, this process does not convert the 1-hour time series data into their respective 1-min time series data, but the process only enhances the rain cell extension plots of the 1-hour data by producing more points. With these new values, the new rain cell size distribution is derived for Durban area as shown in Fig. 4(c). Linear extrapolation is then applied to obtain the percentile level where the rain cell size will have the exact or near exact value as that generated from the 1-min data. This is determined to be the 99.99% centile. This data manipulation is repeated on the 1-hr time series data obtained from all the other locations. In summary, to achieve higher resolution in the measured 1-hour time series rain rate data, we obtain the equivalent time series data that would produce the same CDF as the 1-min data by the use of conversion values in Table 1.

Figure 4(a) is the plot from 1-minute data: when equal advection velocity of 10 m/s is applied uniformly for all cells (see 3 mm/h at 10 m/s), the cell range is more exaggerated than if 6 m/s were used for the stratiform rain cells.

Figure 4(c) illustrates the cell sizes derived from the enhanced 1-hour rain rate data for Durban showing that the largest rain cell extends up to 9 km while the smallest diameter is 2 km in range. The maximum cell has a range of 19 km with the smallest cell being 7 km.

The result is a model expressed by (6) [24]:

$$D = 32.673R^{-0.467} \quad (6)$$

where D (km) is the equivalent rain cell diameter, and R (mm/h) is the rain rate.

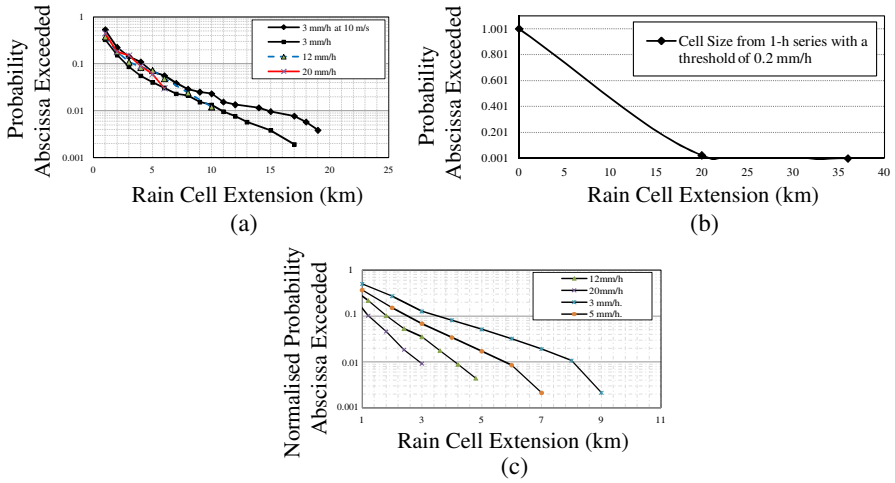


Figure 4. Rain cell size CDF for Durban. (a) Measured 1-min data. (b) Measured 1-h series data. (c) Data series converted from 1-h data.

When this result is compared to the available radar measurements of rain cell sizes, rain rate threshold of 5 mm/h was found to extend up to 25 km in Spinno D’Adda, Italy and Chilbolton, England. This could mean that the data collection from the disdrometer do not fully represent all the rain events in Durban. Also, we have earlier shown that the resulting rain cell diameter of (6) is the weighted mean intercept of the virtual radio path [33]. For worst case consideration of the largest rain cell that occurs, then we multiply the (6) by a factor of $\pi/2$. Thus the model becomes $D = 51.32R^{-0.467}$. When the rain cell statistics from Fig. 4(c) (plotted from the enhanced 1-hr data) is linearly interpolated to the 99.99% percentile and by the use of Goldhirsh method, the new rain cell model is deduced as [24, 26]:

$$D = 51R^{-0.46} \tag{7}$$

This result shows that the 5 mm/h threshold extends up to 24.3 km which is close to the reported radar observations of 25 km.

Figures 5(a) and (b) show the CDF of cell sizes and the Goldhirsh’s method of conversion at 99% centile respectively with data obtained from Richard’s Bay. The same extrapolation is carried out to derive the cell sizes at 99.99% centile.

The resulting model is given as:

$$D = 55R^{-0.455} \tag{8}$$

This procedure was carried out for the eight locations, and the unique coefficients for rain cell sizes are listed in Table 4 since other towns

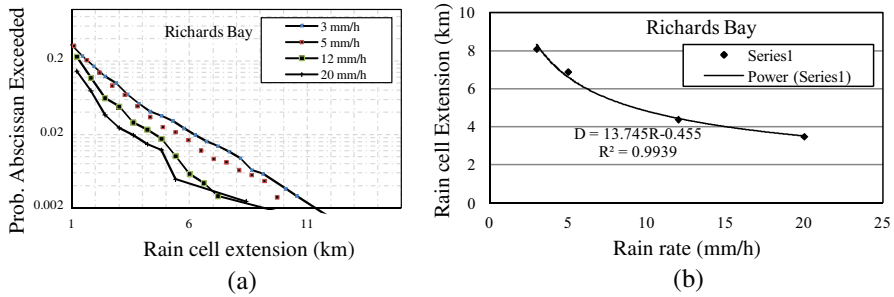


Figure 5. Rain cell diameter (a) CDF for Richard’s Bay. (b) Derivation of rain cell size at 99% percentile.

Table 4. Equivalent rain cell diameter coefficients for some locations in South Africa.

LOCATION	LON	LAT	<i>u</i>	<i>v</i>
DURBAN	29°97'	30°95'	51	−0.460
PRETORIA	25°73'	28°18'	30	−0.462
PIETERMARITZBURG	30°40'	29°63'	45	−0.467
RICHARD’S BAY	32°6'	28°48'	55	−0.455

had the same relationships. The values for *u*-parameter seem to be dependent on the location while the slope-parameter, *v* remains somewhat constant for the region (about 0.461 on average). The rain cell sizes derived in this work do not necessarily refer to the mean cell diameter but rather the maximum cell size that passes through the point rain rate equipment. Rainfall occurs with highly intensive cells embedded in the stratiform structures where their contribution to attenuation on the radio link is obtained from the sum of the input of all the cells. The derived relationships in Table 4 can then be applied in attenuation prediction for the localities of interest and also in site diversity planning as long as the attenuation equation requires the rain cell size as an input. From Table 4, it is noted that the overall rain cell sizes at the coastal areas in the eastern part of the country for example in Durban and Richard’s Bay, are larger than those of the inland areas as in the case of Pretoria and Pietermaritzburg.

4. RAIN ATTENUATION PREDICTION AT 0.01% OF TIME

ITU-R presents a formula for obtaining attenuation due to rain, A for terrestrial links defined as [34]:

$$A = \gamma_s r \cdot L \quad [\text{dB}] \quad (9)$$

where γ is the specific attenuation, r is the reduction factor and L the actual path length of the link.

In another ITU-R recommendation [23], the specific attenuation is computed from the power law rain rate relationship:

$$\gamma_s = k R_{0.01}^\alpha \quad [\text{dB/km}] \quad (10)$$

where k and α are frequency and polarization dependent factors.

In our previous work [33], we derived the path attenuation prediction expressions for a terrestrial link in Durban which are summarized below.

$$A = \frac{\gamma L}{\cos\theta} s \frac{2}{\pi} \left(1 + \frac{1.047}{\xi_\theta} \right) \left(\frac{1}{\xi_\theta L/D + 1} \right) \quad (11)$$

$$s_1 = 1 + (s_m - 1) \exp - \left(\frac{(R - (R_b/\pi))^2}{2\zeta^2} \right) \quad (12)$$

$$s_m = 1.24681 \quad \zeta = 0.6817 R_b \quad (13)$$

$$\eta_\theta = (-0.0001\theta^2 - 0.0029\theta + 1.0175) \quad (14)$$

$$\xi_\theta = \frac{1}{\eta_\theta} \quad (15)$$

where θ is the link elevation angle (may be taken as zero for terrestrial links), s_1 the rain cell growth factor, R_b the break point rain rate (taken to be rain rate exceeded 0.01% of the time), L the length of the whole path, and ξ_θ the link elevation coefficient (almost unity for terrestrial links). The rain cell size, D , is obtained from Table 4 but the distribution for Durban in (7) is recommended.

The value of the rain rate where an abrupt increase in the rain rate growth occurs is the break point value, R_b . This value is easily visualized when high resolution data (e.g., 1-minute integration time) is used to plot the CDF of rain rates. It has been shown that R_b is a value close to the rain rate value equaled or exceeded 0.01% of time, $R_{0.01}$. ITU-R provides rain rate maps for $R_{0.01}$ values around the world which can be used in (11) to estimate the rain attenuation at 0.01% of time.

Since reliability level of 99.99% is common in terrestrial link deployments but with varying path lengths, we compute the specific

attenuation based on the rain rate values exceeded 0.01% of time. We apply the rain rate map deduced by [13, 32] for South Africa to produce the contour map for the specific attenuation. This is done for 15 GHz and 26 GHz as the center frequencies which are highly susceptible to rain attenuation effects and yet they present large bandwidths required for the growing traffic demand. The data used for the rain rate mapping are based on 21 locations in South Africa. The results for specific attenuation for all other locations are derived by the use of inverse distance weighting method (IDW) and implemented in the MATLAB software to determine the matrix of the interpolated values for all the coordinates in South Africa. The matrix is then transformed into contour plots. The resulting contours for the two center frequencies, 15 GHz and 26 GHz are shown in Fig. 6 and Fig. 7 respectively. These two frequencies are considered since there is more demand for higher bandwidth and they offer a better trade-off for the high rain attenuation that occurs on high capacity radio links. Also, some network operators in South Africa have already planned to roll out their terrestrial transmission network on these frequencies and more are expected to do so in the near future. The eastern coast experiences heavy rainfall and the specific attenuation at 0.01% of

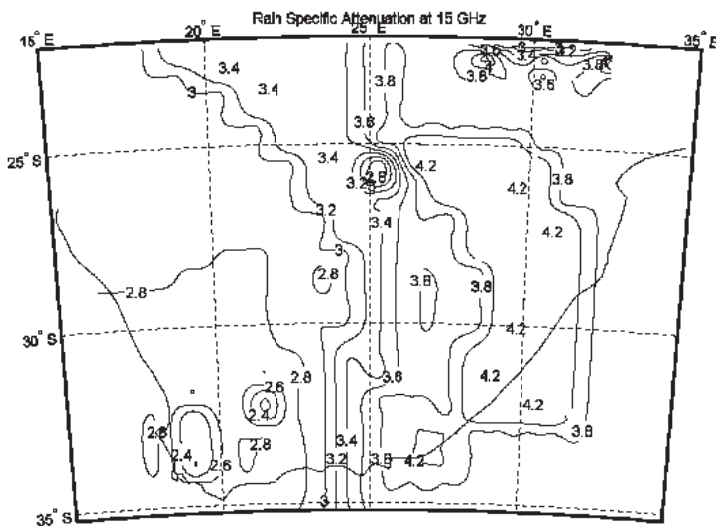


Figure 6. Rain-induced specific attenuation contours for horizontally polarized microwave link at 15 GHz frequency for outage level of 0.01% of the time.

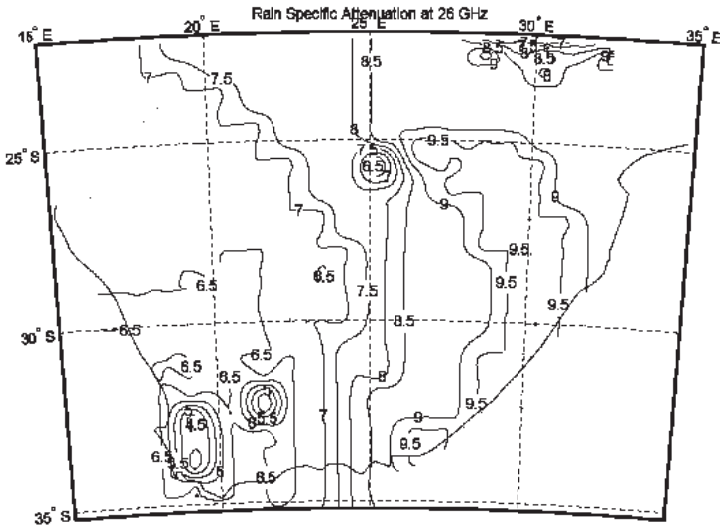


Figure 7. Rain-induced specific attenuation contours for horizontally polarized microwave link at 26 GHz frequency for outage level of 0.01% of the time.

time is 4.2 dB/km. The south western coast which is a temperate zone has lowest values for specific attenuation, 2.4 dB/km. Average values for specific attenuation are obtained in the central parts of the country where rainfall rates lie between the peak and lowest values at the same probability level. With these results and the knowledge of the path length, the expected path attenuation at 0.01% of time can be computed by the use of the expressions (11) through (15).

5. SITE DIVERSITY PLANNING

In terrestrial and satellite link planning, the received signal power level (RSL) is determined from the decibel difference between the equivalent isotropically radiated transmitter power (EIRP) and the total net path loss [34]:

$$RSL = P_t + G_t + G_r - FSL - A_g - L_r - L_t - (A_r + A_w) \quad (16)$$

where P_t is the transmitted power, G_t is the gain of the transmitter, G_r is the receiver gain, Free space loss (FSL), A_g is the attenuation due to gas, A_r is the attenuation due to rain, A_w is the wet antenna loss (both transmitter and receiver terminals), L_t is the loss in transmit-systems and L_r is the loss in the receive-systems.

The gaseous loss is mainly contributed from vapor absorption (0.16 dB/km at 22 GHz) and oxygen absorption (15 dB/km at 60 GHz). The free space loss is derived from the following [34, 35]:

$$\text{FSL} = (32.4 + 20\log_{10}L + 20\log_{10}f) \quad (17)$$

where f (GHz) is the frequency used in the link and L is the link path length in km.

With the knowledge of the rain rate, $R\%$ at desired availability, expected rain attenuation, $A(p)\%$ can be computed. Link planners normally provide a fade margin based on clear weather conditions. In the case of a rain event, the free space loss (FSL) is expected to lessen thus providing for the signal loss in a rain medium. However, this approach leads to low link reliability during rain events and thus the provision for rain attenuation during initial link planning has become necessary. From (16), the rain fade margin can be alleviated by increasing the transmitter equivalent isotropically radiated power (EIRP) and the gain of the receiver. But due to large attenuation margins experienced from rain attenuation, the power and gain adjustments are not sufficient: thus site diversity comes into play.

Two sites in a geographical area may be affected equally by the same rain event that covers that area. With the knowledge of the rain cell extension length for a given rain rate threshold, the minimum distance between two diversity sites can be determined to increase diversity gain. This analysis is presented for both terrestrial and satellite radio links since both links are similar in view of site diversity apart from the fact that the link elevation angle for terrestrial case is normally small. Given two sites w and x that are to be linked by a terrestrial link, this can be done directly as a line of sight (LOS) link. To alleviate the rain fade by site diversity method, the same link can be routed via another site y , then y to w , such that x and y become the two diversity sites.

The mean attenuation for a single site; A_s is expressed as [36]:

$$A_s = \frac{1}{2} \{A_x + A_y\} \quad (18)$$

$$A_J(t) = \text{minimum} [A_x(t) + A_y(t)] \quad (19)$$

where A_x is the attenuation at site x and A_y the attenuation at site y . A_J is the joint attenuation for the two sites.

The diversity gain $G_D(P)$ of attenuation equaled or exceeded at a given percentage of the time, P is given by:

$$G_D(P) = A_s(P)A_J(P) \quad (20)$$

where $A_J(p)$ is the joint attenuation for sites x and y .

Link reliability, Γ is the percentage of time the link is within the received threshold level despite any environmental changes. The percentage, $P\%$ for which a required margin, M_r is equaled or exceeded can be expressed as given in (21a):

$$P = (100\% - \Gamma) \quad (21a)$$

The rain fade margin, M_r

$$M_r = A(P) + \delta N - G_D(P) \quad (21b)$$

$A(P)$ is the expected single site attenuation, and δN is the (thermal) loss due to increase in temperature. Hodge [30, 31] has shown that the diversity gain can be computed from a given attenuation, A and the separation distance, d :

$$G_D = G_d G_f G_E G_z \quad (22)$$

$$G_D = m \left(1 - e^{-nd}\right) \quad (23)$$

$$m = 0.64A - 1.6 \left(1 - e^{-0.11A}\right) \quad (24)$$

$$n = 0.585 \left(1 - e^{-0.98A}\right) \quad (25)$$

$$G_f = 1.64e^{-0.025f} \quad (26)$$

$$G_E = 0.00492\theta + 0.834 \quad (27)$$

$$G_z = 0.00177z + 0.887 \quad (28)$$

where z is the baseline-to-path angle, θ the elevation angle, and f (GHz) the frequency used.

From above, the diversity gain is expected to vary from zero to the maximum (single site attenuation) when d is large enough such that the rain at the two sites are uncorrelated. However, rainfall occurs as stratiform structure with convective rain cells altogether. Therefore there is saturation for site diversity gain, which is a value less than single site attenuation. The distance should not be too large since the next site may fall into another rain region.

From (21a), in order to achieve reliability at $P = 0.01\%$, the diversity gain corresponds to the rain attenuation expected to be equaled or exceeded 0.01% of the time. For Durban, the rain attenuation equaled or exceeded 0.01% of the time, is computed from (11) where the value of rain rate is given as 60 mm/h [32, 33]. From Table 2, the rain rate threshold of 60 mm/h is computed to stretch up to 7.75 km in Durban area. To maximize site diversity gain, the second redundant site y , should be situated at least 8 km away from the site, x . The rain cell size relationships therefore provide the minimum required separation distance required to achieve a given link reliability level. To determine the maximum value of

d that will guarantee availability at equal probability, the field of the next neighbor rain cell must be known. It has been reported that thunderstorms could be separated from one another by 10–30 km [36, 37]. Thus, this range of distances provides the maximum separation distance.

This approach is repeated for several stations in the South African region with the knowledge of the rain rate threshold values at the 0.01% of the time and the distance–rain rate relationships described in Table 2 [13, 32, 33]. Since the data used for the rain rate mapping are based on 21 locations in South Africa, the results for d for all other locations are derived by the use of inverse distance weighting method (IDW) and implemented in the MATLAB software to determine the interpolated distance matrix for all the coordinates in South Africa. The matrix is then transformed into contour plots to depict the rain field extension areas bound by the thresholds at 0.01% of time. The result is shown in Fig. 8 which is applicable for site diversity planning for both terrestrial and satellite high capacity radio links. With the values of d given for the climatic regions of South Africa, link planners will easily apply the equations (22) through (28) to derive the optimal diversity gain. Other recent developments on site diversity topic can be found in studies involving multiple sites [38–43].

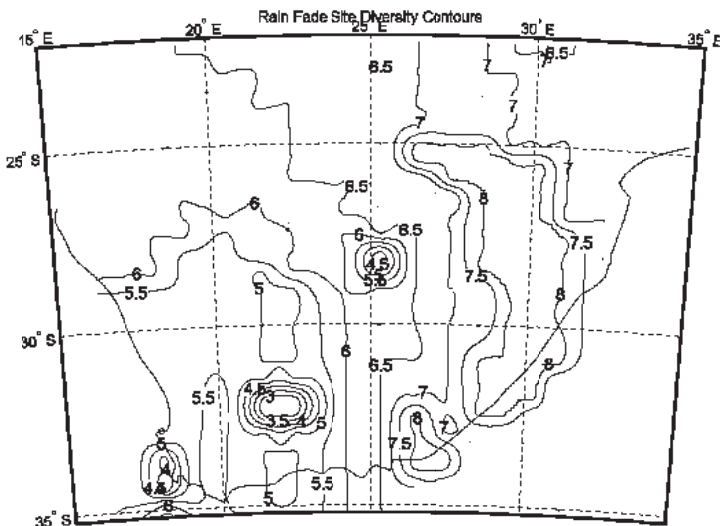


Figure 8. Site diversity distance plot for link reliability of 99.99% in South Africa.

6. CONCLUSION

The rain cell sizes for the South African region have been successfully derived based on point rain rate data collected over five years. There are variations in cell sizes based on the total fractal area of observation and the size of the cells are seen to be directly proportional to the values of rainfall rate measurements at 0.01% of time.

The applications for the cell sizes have been introduced as applied in attenuation prediction and site diversity planning. Unless 1-minute data measurements are carried out throughout the country and rain cells sizes derived, the results in this work present a viable solution to the need. Since the rain cell size derivation process is based on the assumption of velocity of advection, which varies for the stratiform and convective rain forms, comparison of rain fields from RADAR data and from a network of point rain rate equipment is recommended for further analysis.

REFERENCES

1. ITU-R P.837-5-2007, "Characteristics of precipitation for propagation modeling," Geneva, 2007.
2. Crane, R. K., "Prediction of attenuation by rain," *IEEE Trans. Comm.*, Vol. 28, 1717–1733, 1980.
3. Crane, R. K., *Electromagnetic Wave Propagation Through Rain*, 1–40, John Wiley, New York, 1996.
4. Ajayi, G. O., S. Feng, S. M. Radicella, and B. M. Reddy, *Handbook on Radio Propagation Related to Satellite Communications in Tropical and Subtropical Countries*, 7–14, ICTP, Trieste, 1996.
5. Ojo, J. S., M. O. Ajewole, and S. K. Sarkar, "Rain rate and rain attenuation prediction for satellite communication in Ku and Ka bands over Nigeria," *Progress In Electromagnetics Research B*, Vol. 5, 207–233, 2008.
6. Moupfoma, F., "Improvement of a rain attenuation prediction method for terrestrial microwave links," *IEEE Transactions on Antennas and Propagation*, Vol. 32, 1368–1372, 1984.
7. Ajayi, G. O. and E. B. C. Ofoche, "Some tropical rainfall rate characteristics at Ile-Ife for microwave and millimeter wave application," *J. of Climate and Applied Meteor.*, Vol. 23, 562–567, 1983.

8. Watson, P. A., M. Gunes, B. A. Potter, B. Sasthiaseelan, and J. Leitas, "Development of a climatic map of rainfall attenuation for Europe," Post Graduate School of Electrical and Electronic Engineering, University of Bradford, No. 327, 153, 1982.
9. Moupfouma, F., "Rainfall-rate distribution for radio system design," *IEE Proceedings*, Vol. 134, No. 6, 527–537, Feb. 1987.
10. Mulangu, C. T., P. A. Owolawi, and T. J. Afullo, "Rainfall rate distribution for LOS radio systems in Botswana," *SATNAC Conference*, Mauritius, Sept. 2007.
11. Fashuyi, M. O., P. A. Owolawi, and T. O. Afullo "Rainfall rate modelling for LoS radio systems in South Africa," *Trans. of South African Inst. of Elect. Engineers*, Vol. 97, 74–81, 2006.
12. Odedina, M. O. and T. J. Afullo, "Characteristics of seasonal attenuation and fading for line-of-sight links in South Africa," *Proc. of SATNAC*, 203–208, Sept. 2008.
13. Owolawi, P. A., "Rain rate probability density evaluation and mapping for the estimation of rain attenuation in South Africa and surrounding Islands," *Progress In Electromagnetics Research*, Vol. 112, 155–181, 2011.
14. Flavin, R. K., "Rain attenuation considerations for satellite paths," *Australian Telecomm. Research*, Vol. 23, No. 2, 4755, 1982.
15. Segal, B., "The influence of rain gauge integration time on measured rainfall-intensity distribution functions," *J. of Atmospheric and Oceanic Tech.*, Vol. 3, 662–671, 1986.
16. Rice, P. and N. Holmberg, "Cumulative time statistics of surface-point rainfall rate," *IEEE Trans. Commun.*, Vol. 21, 1772–1774, Sept. 2002.
17. Singh, M. S., K. Tanaka, and M. Lida, "Conversion of 60-, 30-, 10- and 5-minute rain rates to 1-minute rates in tropical rain rate measurement," *ETRI Journal*, Vol. 29, No. 4, Aug. 2007.
18. Karasawa, Y. and T. Matsudo, "Prediction of one-minute rain rate distribution in Japan," *Trans. IEICE*, 518–527, 1990.
19. Capsoni, C. and L. Luini, "A physically based method for the conversion of rainfall statistics from long to short integration time," *IEEE Transactions on Antennas and Propagation*, Vol. 57, No. 11, 2009.
20. Emiliani, L. D., L. Luini, and C. Capsoni, "Analysis and parameterization of methodologies for the conversion of rain-rate cumulative distributions from various integration times to one minute," *IEEE Antennas Propag. Mag.*, Vol. 51, No. 3, 70–84, Jun. 2009.

21. Owolawi, P. A., T. J. O. Afullo, and S. B. Malinga, "Rainfall rate characteristics for the design of terrestrial link in South Africa," *Proc. of SATNAC*, 71–76, Sept. 2008.
22. Owolawi, P. A. and T. J. O. Afullo, "Rainfall rate modeling and worst month statistics for millimetric line-of-sight radio links in South Africa," *Radio Science*, Vol. 42, 2007.
23. ITU-R P.838-3-2005 "Specific attenuation model for rain for use in prediction methods," Geneva, 2005.
24. Akuon, P. O. and T. J. O. Afullo, "Rain cell size statistics from rain gauge data for site diversity planning and attenuation prediction," *Proc. of SATNAC*, 213–216, East London, South Africa, Sept. 4–7, 2011.
25. Drufuca, G. and G. I. Zawadzki, "Statistics of rain gauge data," *J. of Applied Meteorology*, Vol. 14, 1419–1429, Dec. 1975.
26. Goldhirsh, J., "Rain cell statistics as a function of rain rate for attenuation modeling," *IEEE Transactions on Antennas and Propagation*, Vol. 57, No. 5, 799–801, Sept. 1983.
27. Pawlina, A., "No rain intervals within rain events: Some statistics based on Milano radar and rain-gauge data," COST Action 280, 1st International Workshop, Jul. 2002.
28. Begum, S., C. Nagaraja, and I. Otung, "Analysis of rain cell size distribution for application in site diversity," *IEEE Transactions on Antennas and Propagation*, 1–5, 2006.
29. Matriccioni, E. and A. P. Bonati, "Rain cell size statistics inferred from long term point rain rate: Model and results," *Proc. Third Ka Band Utilization Conference*, Sorrento, Italy, Sept. 1997.
30. Hodge, D. B., "An empirical relationship for path diversity gain," *IEEE Transactions on Antennas and Propagation*, Vol. 24, 250–251, Mar. 1976.
31. Hodge, D. B., "An improved model for diversity gain on earth-space propagation paths," *Radio Science*, 17, 1379–1399, Nov.–Dec. 1982
32. Owolawi, P. A., "Characteristics of rain at microwave and millimetric bands for terrestrial and satellite links attenuation in South Africa and surrounding islands," Ph.D. Thesis, School of Electrical, Electronic & Computer Engineering, University of KwaZulu-Natal, Durban, July 2010.
33. Akuon, P. O. and T. J. O. Afullo, "Path reduction factor modeling for terrestrial links based on rain cell growth," *Proceedings of IEEE Africon Conference*, Livingstone, Zambia, Sept. 12–15, 2011.

34. Freeman, R. L., *Radio System Design for Telecommunication*, 3rd edition, A Wiley Interscience Publication, John Wiley & Sons Inc., 2007.
35. Recommendation ITU-R 530-10, "Propagation prediction techniques and data required for the design of terrestrial line-of-sight systems," *International Telecommunication Union*, Vol. 2001, 271–295, P Series, Geneva, Switzerland, 2001.
36. Pratt, T. and C. W. Bostian, *Satellite Communications*, 345–346, A Wiley Interscience Publication, John Wiley & Sons Inc., 1988.
37. Pawlina, A. A., "No rain intervals within rain events: Some statistics based on Milano radar and rain-gauge data," *Propagation Impairment Mitigation for Millimetre Wave Radio Systems*, COST Action 280, 1st International Workshop, Jul. 2002.
38. Panagopoulos, A. D., P. M. Arapoglou, J. D. Kanellopoulos, and P. G. Cottis, "Long term rain attenuation probability and site diversity gain prediction formulas", *IEEE Transactions on Antennas and Propagation*, Vol. 53, No. 7, Jul. 2005.
39. Sakarellos, V. K., D. Skraparlis, A. D. Panagopoulos, and J. D. Kanellopoulos, "Outage performance analysis of a dual-hop radio relay system operating at frequencies above 10 GHz," *IEEE Transactions on Communications*, Vol. 58, No. 11, Nov. 2010.
40. Panagopoulos, A. D. and J. D. Kanellopoulos, "Prediction of triple-orbital diversity performance in earth-space communication," *International Journal of Satellite Communications*, No. 20, 187–200, 2002.
41. Panagopoulos, A. D. and J. D. Kanellopoulos, "Adjacent satellite interference effects as applied to the outage performance of an earth-space system located in a heavy rain climatic region," *Annals of Telecommunications*, No. 9–10, 925–942, 2002.
42. Matricciani, E., "Physical-mathematical model of the dynamics of rain attenuation based on rain rate time series and two layer vertical structure of precipitation," *Radio Science*, Vol. 31, No. 2, 281–295, 1996.
43. Matricciani, E., "Prediction of orbital diversity performance in satellite communication systems affected by rain attenuation," *Intern. Journal of Satellite Communications*, Vol. 15, 45–50, 1997.